Bioorganic & Medicinal Chemistry 20 (2012) 1494–1501

Contents lists available at SciVerse ScienceDirect

Bioorganic & Medicinal Chemistry

journal homepage: www.elsevier.com/locate/bmc

Chemical reactivity and microbicidal action of bethoxazin

Gaik-Lean Chee [a,*], Bharat Bhattarai [a], R. Daniel Gietz [b], Samaa Alrushaid [a], John L. Nitiss [c], Brian B. Hasinoff [a]

[a] Faculty of Pharmacy, University of Manitoba, Winnipeg, Canada R3E 0T5
[b] Department of Biochemistry and Medical Genetics, Faculty of Medicine, University of Manitoba, Winnipeg, Canada R3E 0J9
[c] Department of Molecular Pharmacology, St. Jude Children's Research Hospital, Memphis, TN 38105, USA

ARTICLE INFO

Article history:
Received 7 November 2011
Revised 19 December 2011
Accepted 23 December 2011
Available online 5 January 2012

Keywords:
Bethoxazin
Microbicide
Electrophilicity
Sulfhydryl binding
Topoisomerase II
Yeast

ABSTRACT

Bethoxazin is a new broad spectrum industrial microbicide with applications in material and coating preservation. However, little is known of its reactivity profile and mechanism of action. In this study, we examined the reactivity of bethoxazin toward biologically important nucleophilic groups using UV–vis spectroscopy and LC–MS/MS techniques and found the molecule to be highly electrophilic. Bethoxazin reacted with molecules containing free sulfhydryl groups such as GSH and human serum albumin to form covalent adducts that were detectable by MS, but did not react with amino, carboxylic, phenolic, amino oxo, alcoholic, and phosphate functional groups. Bethoxazin potently inhibited the catalytic activity of yeast DNA topoisomerase II and the growth of yeast BY4742 cells at low micromolar concentrations. However, the reduced form of bethoxazin and GSH-treated bethoxazin were both inactive in these assays. The experimentally determined relative reactivity of bethoxazin and its reduced form analog correlated with their biological activities as well as their quantum-mechanically calculated electrophilicity properties. Taken together, the results suggest that bethoxazin may exert its microbicidal action by reacting with sensitive endogenous sulfhydryl biomolecules of microbial cells. Consistent with this view, the inhibitory activity of bethoxazin on topoisomerase II may be due to its ability to react with critical free cysteine sulfhydryl groups on the enzyme. Our studies have provided for the first time a better understanding of the reactivity of bethoxazin, as well as some insights into the mechanism by which the compound exerts its microbicidal action.

1. Introduction

Bethoxazin (Bethoguard™, **1** in Fig. 1) is a broad spectrum industrial microbicide introduced by Janssen Pharmaceutica[1] and registered with the US Environmental Protection Agency (code 090421) in 2006 for use in woods to control the growth of fungi, molds and algae. It is also being promoted for use as a preservative in plastics, stains, adhesives and sealants.[2] The compound was originally discovered by the Uniroyal Chemical Crop Protection Division in the early 1990s as a fungicide that exhibited high potency against certain fungal pathogens in vitro.[3,4] However, the compound did not exhibit any promising activity in eradicating or preventing fungal infection in plants (company's unpublished results), and as a result, bethoxazin was not further developed for use on crops.

The mechanism by which bethoxazin exerts its microbicidal action and other toxicities is unknown. It is also unclear why bethoxazin is much less effective in controlling fungal diseases in plants. Studies on bethoxazin have focused mostly on the evaluation of its biocidal activity spectrum for commercial purposes.[1–7] An understanding of the reactivity of bethoxazin should provide some insight into the mechanism of action of the molecule, and help define the formulations and conditions required for practical application of the compound.

Bethoxazin has a 1,4,2-oxathiazine 4-oxide ring system that is relatively uncommon (Fig. 1). A search in SciFinder Scholar (CAS, Columbus, OH) indicates that this ring is not found in the structures of any commercially available compounds and is found in only 134 other structures. Therefore, because the chemistry of oxathiazine oxide ring system has not been closely examined, a study of the reactivity of bethoxazin should provide a better understanding of the chemical and biological properties of this ring system.

The oxathiazine oxide ring of bethoxazin (Fig. 1) consists of a sp^2-hybridized carbon, C3, that may be susceptible to nucleophilic attack. The hypothesis is made on the basis that atom C3 is attached to an electronegative oxygen (O1) and a strongly

Abbreviations: Cys, cysteine; DTT, dithiotreitol; ESI, electrospray ionization; GSH, glutathione; HRMS, high resolution mass spectrometry; HSA, human serum albumin; kDNA, kinetoplast plasmid DNA; k_{obs}, pseudo first order rate constant; LC, liquid chromatography; MS, mass spectrometry; MS/MS, tandem mass spectrometry; MSDS, material safety data sheet; $t_{1/2}$, half-life; Tris, tris(hydroxymethyl)aminomethane; UV–vis, ultraviolet–visible.

* Corresponding author. Tel.: +1 204 272 1589; fax: +1 204 474 7617.
E-mail address: lean_chee@umanitoba.ca (G.-L. Chee).

0968-0896/$ - see front matter © 2012 Elsevier Ltd. All rights reserved.
doi:10.1016/j.bmc.2011.12.051

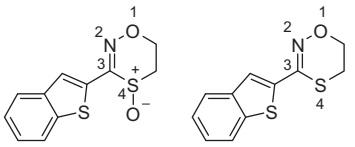

Figure 1. Chemical structures of bethoxazin (**1**) and its reduced form analog (**2**).

electron-withdrawing sulfoxide group at position-4, which could also be a good leaving group. The hypothesis is also supported by the longer than usual S4–C3 bond as reported in the X-ray crystal structure of bethoxazin.[5] In addition to atom C3, the sulfoxide group itself in the oxathiazine oxide ring of bethoxazin may also be electrophilic. This is suggested because DMSO ($Me_2S^+O^-$) has been found to react slowly with sulfhydryl nucleophiles such as methanethiol to form a sulfurane intermediate ($Me_2(MeS)SOH$)[8] despite the fact that a sulfoxide is better known to react with an electrophile (R′X) to form a sulfonium ion intermediate ($R_2S^+OR'{\cdot}X^-$).[9] The hypothesis that bethoxazin may be electrophilic is further supported by chemical decomposition of bethoxazin at high pH,[1] which may involve nucleophilic attack of bethoxazin by hydroxide anions.

Based on the above reasoning, we examined the reactivity of bethoxazin towards a representative set of nucleophilic functional groups present in the biological systems. The relationship between chemical reactivity and biological activity of bethoxazin and its reduced form, analog **2** (Fig. 1),[4] was explored to explain the microbicidal mechanism of bethoxazin. Reaction products were also characterized to test our hypothesis on the electrophilicity of C3 in an oxathiazine ring as well as to propose the reaction mechanism for nucleophilic attack on the molecule.

2. Experimental

2.1. Materials, yeast cells and enzyme

Bethoxazin and analog **2** were gifts from Chemtura (Guelph, Canada). Reagents used as nucleophiles were GSH, cysteine, HSA, sodium acetate, methanol, phenol, alanine methyl ester, guanine, and methyl 3-mercaptopropionate were from Sigma–Aldrich (Oakville, Canada). The yeast cells (BY4742 strain, MATalpha his3Δ1 leu2Δ0 lys2Δ0 ura3Δ0) were from Open BioSystems (Hunstville, AL). Recombinant yeast topoisomerase II enzyme was purified using a protease-deficient topoisomerase I-negative strain JEL1t1 as we previously described.[10]

2.2. Chemical stability studies

The reactions of bethoxazin and **2** with a nucleophile were carried out at room temperature or 37 °C as indicated and followed spectrophotometrically by repeated scanning, at fixed times, on a Cary 1 spectrophotometer (Varian, Mulgarave, Australia). The reactions were initiated by adding a small volume of stock nucleophiles to a freshly prepared 30–100 μM of bethoxazin or **2** in 20 mM Tris or phosphate buffer solution at pH 5.4 or 7.4, as indicated, to give a total volume of 1 mL in 1 cm stoppered silica cells.

2.3. LC–MS/MS analysis of bethoxazin-GSH reaction products

Two equivalents of GSH were added to 100 μM of bethoxazin in 20 mM Tris buffer (pH 7.4) containing 10% (v/v) methanol. The reaction was allowed to proceed at room temperature for 8 h and then diluted twofold to give a 50% (v/v) methanol/aqueous solution. In a separate experiment, the same reaction was performed with 2.1 equiv of GSH in 20 mM Tris buffer (pH 7.4) without using methanol as a co-solvent and was diluted to give a 50% (v/v) methanol/aqueous solution as described before. Both solutions were subsequently analyzed on a Varian 500-MS LC–MS/MS ion trap mass spectrometer (Mississauga, Canada) equipped with 212-LC chromatography equipment. The eluent used was 80% (v/v) methanol/water containing 0.1% (v/v) formic acid for the first 5 min, which was changed to 90% (v/v) methanol/water over 2 min and maintained for the remaining 21 min of the run. The eluent flow rate was 200 μL/min and the sample (10 μL) was chromatographed on a Varian Pursuit C-18 column (3 μm pore size, 100 × 2 mm). The ionization mode was positive ESI with N_2 at 35 psi as the nebulizer gas. The drying gas was set at 18 psi and 350 °C. The voltages of the needle and shield were 4059 and 90 V, respectively. Positive ions were scanned in the range of 200–900 Da using a scan rate of 15 kDa/s and a mass increment of 150–2000 Da. The relevant precursor ions were selected for low energy collision-induced dissociation MS/MS analyses using helium as the collision gas with a flow rate of 0.8 mL/min and collision voltage in the range of 0.5–2.5 V.

2.4. Reaction of bethoxazin with methyl 3-mercaptopropionate

A 100 mM solution of methyl 3-mercaptopropionate in DMSO (210 μL, 210 μM) was added to 100 μM of bethoxazin in 20 mM of Tris buffer (100 mL, pH 7.4). The resulting mixture was stirred at room temperature for 8 h before it was extracted with ethyl acetate (20 mL). The organic phase was dried (Na_2SO_4) and concentrated under reduced pressure to afford a colorless residue (3.2 mg). The ^1H and ^{13}C NMR spectra of the product were recorded at 300 K on a Bruker AM-300 FT NMR spectrometer (Bruker, Milton, Canada) operating at 300.13 MHz and 75.5 MHz, respectively. The ESI-MS was recorded on a Varian 500-MS ion trap mass spectrometer. The HRMS was recorded on a Bruker micrOTOF ESI-Time-of-Flight MS system. ^1H NMR ($CDCl_3$) δ 7.77 (2H, m), 7.73 (1H, s), 7.38 (2H, m), 4.54 (2H, t, J = 6.5), 3.71 (3H, s), 3.69 (3H, s), 3.35 (2H, t, J = 7.2), 3.09 (2H, t, J = 6.5), 2.97 (2H, t, J = 7.2), 2.79 (2H, t, J = 7.2), 2.67 (2H, t, J = 7.2); ^{13}C NMR ($CDCl_3$) δ 172.16 (C), 171.83 (C), 145.32 (C), 140.49 (C), 139.01 (C), 138.20 (C), 126.38 (CH), 125.81 (CH), 124.64 (CH), 124.41 (CH), 122.27 (CH), 72.97 (CH_2), 51.90 (2 × CH_3), 37.51 (CH_2), 35.06 (CH_2), 33.98 (CH_2), 33.36 (CH_2), 28.14 (CH_2); ESI-MS m/z (relative intensity) 496 ($[M+Na]^+$, 100), 337 (10), 307 (8); HRMS calcd for $[C_{19}H_{23}NO_5S_4+H]^+$ 474.0537, found 474.1049.

2.5. ESI-MS study of bethoxazin binding to HSA

The reaction of bethoxazin with HSA was carried out by adding 11 μL of 6 mM bethoxazin (66 μM final concentration) in DMSO to 1 mL of 65 μM HSA in 16 mM Tris buffer (pH 7.4) under sterile conditions. The reaction was allowed to proceed at 37 °C for 5 h, and the resulting mixture was then dialyzed three times in water (1 L) for 2 h at 4 °C using a dialysis membrane with a 10,000 Da cutoff to remove non-covalently or weakly bound small molecules. Water (124 μL), methanol (76 μL), and formic acid (17 μL, 6% (v/v)) were added to the dialyzate (150 μL) prior to MS analysis on an Applied Biosystems API 2000 Triple Quadrupole mass spectrometer (Thornhill, Canada) equipped with a syringe pump (Harvard Apparatus, Holliston, MA) at a flow rate of 5–10 μL/min. The Analyst software (version 1.4) was used for system control and data acquisition. The ESI source was operated in the positive ion mode with an electrospray voltage of +4.4 kV, without capillary heating. Scanning was 1000–1800 *m/z* units every 4 s with a step size of 0.10 amu. MagTran freeware (version 1.02, http://www.geocities.com/SiliconValley/Hills/2679/magtran.html) was used for

charge state deconvolution of HSA and HSA treated with bethoxazin.

2.6. Yeast DNA topoisomerase II decatenation inhibition gel assay

The catalytic inhibition of topoisomerase II by bethoxazin, **2**, and GSH-treated bethoxazin was measured by the ATP-dependent decatenation of kDNA (Topogen, Port Orange, Fl) into minicircles of DNA using a procedure we previously described.[11] For the GSH-treated bethoxazin sample, 100 μM of bethoxazin in 20 mM of Tris buffer (pH 7.4) was treated with 2.1 equiv of GSH for 8 h at room temperature and then concentrated to dryness under reduced pressure before it was dissolved in DMSO and used in the enzyme assay. The enzymatic reactions were carried out in 20 μL volume and contained 50 mM Tris–HCl (pH 8.0), 120 mM KCl, 10 mM $MgCl_2$, 0.5 mM ATP, 30 μg/mL bovine serum albumin, 40 ng kDNA, 0.5 μL compound or DMSO, and 75 ng yeast topoisomerase II protein. The reaction was allowed to proceed at 37 °C for 20 min and terminated by the addition of 6 μL of a stop buffer containing 5 mM Tris pH 8.0, 30% (w/v) sucrose, 0.25% (w/v) bromophenol blue, and 125 mM Na_2EDTA. The decatenated reaction products were loaded on to a 1% (w/v) agarose gel containing 0.5 μg/mL of the DNA stain ethidium bromide and separated using a running buffer containing 40 mM Tris–HCl, 2 mM Na_2EDTA, and 0.11% (v/v) glacial acetic acid at 80 V for about 50 min. The DNA in the gel was imaged by its fluorescence on an Alpha Innotech (San Leandro, CA) Fluorochem 8900 imaging system equipped with a 365 nm UV illuminator and charge-coupled device camera.

2.7. Yeast growth inhibition assay

Yeast BY4742 cells were grown overnight in 5 mL of YPAD liquid medium containing 1% Bacto yeast extract (BD Diagnostics, Mississauga, Canada), 2% Bacto peptone (BD Diagnostics), 2% dextrose and 100 mg/l adenine hemisulfate. The cell density was determined using a hemocytometer. The titer of the YPAD culture was inoculated at a cell density of 5×10^6 cells/mL and 100 μL was delivered into each well of a 96-well plate. Bethoxazin, **2**, and GSH-treated bethoxazin sample were dissolved in DMSO and added to the wells such that the final concentration of DMSO was 0.5% (v/v). The GSH-treated bethoxazin sample was prepared as described above in the topoisomerase II assay section. The plates were incubated for 6 h at 30 °C with shaking at 200 rpm at which time 7 μL of 3-(4,5-dimethylthiazol-2-yl)-5-(3-carboxymethoxyphenyl)-2-(4-sulfophenyl)-2*H*-tetrazolium (MTS) Cell Titer 96 Aqueous One Solution (Promega, Madison, WI) was added to each well and incubated for a further 4 h, and then stored at 4 °C until absorbance was read. The absorbance was measured in a Molecular Devices (Menlo Park, CA) plate reader. The spectrophotometric 96-well plate cell growth inhibition assay measures the ability of the cells to enzymatically reduce MTS. Three replicates were measured at each drug concentration, and the IC_{50} values and their SEs for growth inhibition were obtained by fitting the absorbance-drug concentration data to a four-parameter logistic equation using Sigma Plot (SyStat, Point Richmond, CA) as we previously described.[11] The errors quoted for the IC_{50} values are standard errors from the non-linear least-square analyses.

2.8. Computational studies of bethoxazin and analog 2

Calculations of molecular orbital properties (HOMO and LUMO) were performed on the lowest energy conformer of bethoxazin and analog **2**. The conformers were identified by a conformational search at ground state using molecular mechanics (MMFF) on Spartan 04 version 1.0.0 software (Wavefunction, Irvine, CA). Single point energy in water was calculated for these conformers using AM1 Hamiltonian and restricted Hartree-Fock formalism on TSAR™ version 3.3 software (Oxford Molecular, Oxford, UK).

3. Results

3.1. Spectrophotometric studies of the reactions of bethoxazin and analog 2 with nucleophiles

Since bethoxazin has the potential to act as an electrophile, its chemical reactivity was first examined with a group of biologically relevant nucleophiles. The study would indicate whether bethoxazin has the ability to form covalent adducts with biomolecules such as peptides, proteins, DNA, and membrane lipids.

The reactivity of analog **2** (Fig. 1), which is a reduced form of bethoxazin and a synthetic precursor in the preparation of bethoxazin,[4] was also examined. It was of interest to include **2** in our studies because the compound is structurally analogous to bethoxazin, but was much less effective than bethoxazin as a wood preservative (Uniroyal Chemical's unpublished results). Therefore, knowing the reactivity of **2** in comparison to bethoxazin could help explain the mechanism of action of bethoxazin.

The reactions of bethoxazin and analog **2** with nucleophiles in Tris buffer at pH 7.4 and 5.4 were followed spectrophotometrically with time. Representative UV–vis spectral changes and plots of absorbance at 327 nm with time, as well as a summary of the k_{obs} and $t_{1/2}$ of the reactions are presented in Figure 2A–F.

Bethoxazin reacted rapidly with five equivalents of GSH and cysteine in Tris buffer (pH 7.4, 25 °C) at about the same rate, giving $t_{1/2}$ values of 2.1 and 1.5 min, respectively (Fig. 2E and F). The reactions with GSH and cysteine displayed an isosbestic point at 317 nm, as shown in Figure. 2A and B, respectively, indicating the formation of a single absorbing product in each reaction. When the reaction with GSH was carried out at pH 5.4, the rate constant was about 86-fold lower than that at pH 7.4 (Fig. 2E and F). The 86-fold decrease in the reaction rate constant corresponds to the theoretical 100-fold decrease in the GSH thiolate anion concentration in going from pH 7.4 to 5.4, which suggests that the thiolate anion was the reactive species. Given that thiolate anion is a much stronger nucleophile than the unionized form, this observation strongly suggests that bethoxazin was reactive only toward strong nucleophiles. A much slower reaction was observed for the reaction of bethoxazin with HSA at pH 7.4 (Fig. 2C). Because the disappearance of bethoxazin in this reaction at 25 °C was too slow to be conveniently followed to completion, a linear fit to the first 60 min of the reaction was performed to obtain the initial rate of reaction from the slope of the fitted line. Assuming that change in the extinction coefficient for the HSA reaction was the same as that for the cysteine reaction, the rate constant of the reaction with HSA was 410-fold lower than that of the reaction with cysteine carried out under the same conditions (Fig. 2F). Since HSA contains a single free cysteine sulfhydryl group that is more sterically hindered than the low molecular weight sulfhydryl compounds, it would be expected to react more slowly with bethoxazin.

In contrast to bethoxazin, **2** did not react with GSH, cysteine, or HSA at pH 7.4 or 5.4 as indicated by the lack of spectral changes over a period of 1 d after the addition of the nucleophiles (Fig. 2D). The absence of an electron-withdrawing sulfoxide group in the oxathiazine ring of **2** substantially reduced the electrophilicity of the molecule.

In contrast to its reactivity toward sulfhydryl groups, bethoxazin did not react with five equivalents of alanine methyl ester, sodium acetate, phenol, and guanine in Tris buffer (pH 7.4) as the reactions displayed no spectral changes over 1 d. Bethoxazin also did not react with phosphate buffer (20 mM, pH 7.4) or methanol (10% (v/v)) in Tris buffer (pH 7.4). Analog **2** also did not react

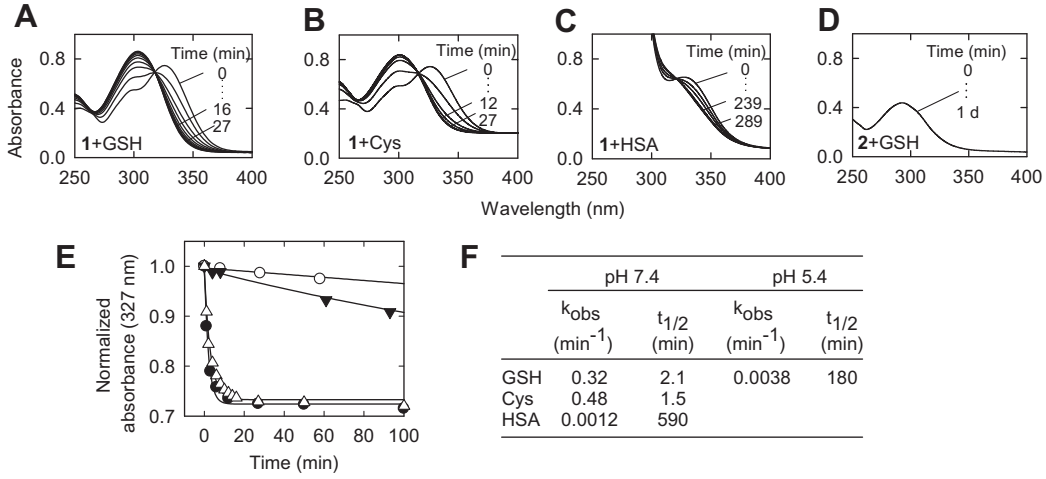

Figure 2. Spectrophotometric study of the reactions of bethoxazin with GSH, cysteine, and HSA, and the reaction of analog **2** with GSH. The spectra were recorded before the addition of the sulfhydryl nucleophile (0 min) and at various times after the addition of the nucleophile. Spectral changes that occurred when 30 μM of bethoxazin was allowed to react with 150 μM of (A) GSH, (B) cysteine, and (C) HSA in 20 mM Tris buffer (pH 7.4, 25 °C). (D) No absorbance changes were observed for analog **2** (100 μM) in 20 mM Tris buffer (pH 7.4, 25 °C) over a 1 d period after the addition of GSH (500 μM), indicating that **2** did not react with GSH. (E) The decrease in absorbance of bethoxazin in the presence of GSH (△), cysteine (●), and HSA (○) at pH 7.4, and GSH (▼) at pH 5.4 were compared by plotting the absorbance at 327 nm with time for each nucleophile. The solid lines for GSH and cysteine at either pH 7.4 or 5.4 are curve fits to a three-parameter exponential decay equation, whereas that for HSA is a linear fit for the first 60 min of the reaction. For comparison purpose, the absorbance for all the reactions was normalized to a value of 1.0 at time 0 min. (F) Summary of k_{obs} derived from the curve fits described in (E) and $t_{1/2}$ values calculated from k_{obs}.

with any of these nucleophiles, which is anticipated given that it did not react with GSH and cysteine. These results suggest that bethoxazin is unlikely to form covalent adducts with biomolecules by reacting with the amino, carboxylic, phenolic, amino oxo, alcoholic, and phosphate functional groups. However, the reaction of bethoxazin with free sulfhydryl groups in peptides and proteins would likely be the major route of reaction for bethoxazin in cells.

3.2. Spectrophotometric determination of the stoichiometry of bethoxazin-GSH binding

To further explore the mechanism of the reaction of bethoxazin with sulfhydryl groups, we determined the stoichiometry of the reaction. The reactions of bethoxazin with 0, 1.1, 2.1, and 5.1 -mol equiv of GSH in Tris buffer (pH 7.4) were carried out at room temperature for 1 h to ensure that the reactions were complete before their UV–vis spectra were acquired. Increasing the molar equivalents of GSH from 0 to 2.1 resulted in spectral changes that were the same as those shown in Figure 2A, displaying an isosbestic point at 317 nm. No further spectral changes were observed when the molar equivalents of GSH were increased to 5.1 from 2.1. The result suggests that bethoxazin reacted with GSH at a ratio of two GSH per molecule of bethoxazin. The isosbestic point observed suggests that a single absorbing product was formed and its formation was independent of the molar equivalents of GSH.

3.3. Characterization of the reaction of bethoxazin with small sulfhydryl molecules

The reactions of bethoxazin with free sulfhydryl groups were further investigated by characterizing the products of bethoxazin-GSH reaction using LC–MS/MS. In the first experiment, the reaction of bethoxazin was carried out with 2.0 equiv of GSH in Tris buffer (pH 7.4) containing 10% (v/v) methanol to prevent the precipitation of bethoxazin. The reaction afforded a major faster-running peak, **I**, and a minor slower-running peak, **II**, in the total ion chromatogram shown in Figure 3A. However, when the reaction was carried out with 2.1 equiv of GSH in Tris buffer without using methanol as a co-solvent, only peak **I** was observed (Fig. 3B). Based on ESI-MS/MS positive mode analysis, peak **I** is proposed to be adduct **4**, which has two molecules of GSH conjugating with one molecule of bethoxazin, resulting from the attack of GSH on atom C3 initially, as shown in Route A of Figure 4. However, we could not rule out peak **I** being adduct **4a** at this stage because S4 of the sulfoxide group of bethoxazin might also be the site of GSH attack as shown in Route B of Figure 4. Structures **4** and **4a** have the same molecular mass and correspond to the molecular ion *m/z* 848 shown in Figure 3C. Both structures are consistent with the finding that the reaction occurred at a ratio of two GSH per molecule of bethoxazin as shown in the stoichiometric determination study. The appearance of two major daughter ions, *m/z* 719, and 701, in the MS/MS fragmentation of *m/z* 848 (Fig. 3D) is consistent with the possible structures proposed for **4** and **4a**. Daughter ion *m/z* 719 was likely resulted from the loss of a glutamyl residue from the parent ion, whereas *m/z* 701 was due to the further loss of a hydroxyl group from daughter ion *m/z* 719, as shown by the proposed fragmentations of structure **4** exemplified in Figure 5.

To confirm the structural identity of peak **I**, we carried out a separate reaction involving bethoxazin and methyl 3-mercaptopropionate, a structurally much simpler GSH analog. We decided to use methyl 3-mercaptopropionate in place of GSH as a model in this study to simplify the product isolation and NMR interpretation. Spectroscopic characterization of this product (data in Section 2.4) revealed adduct **6**, which is a ring opened disulfide structure with two methyl 3-mercaptopropionate molecules attached to it (Fig. 5). Based on this finding, it is reasonable to assign structure **4** to peak **I**, and conclude that the reaction of bethoxazin with GSH occurred with GSH attacking C3 of the oxathiazine oxide ring to form ring opened intermediate **3** (Route A of Fig. 4). Subsequent attack at the sulfenic group of **3** by a second GSH afforded **4** as final product. The formation of disulfide **4** is also supported by a recent report that transiently formed sulfenic acids react with sulfhydryl nucleophiles to give disulfide adducts in good yields.[12] Sulfhydryl attack at C3 was somewhat anticipated because reactions involving sulfhydryl attack at the sulfur atom of a sulfoxide group are rare and have never been reported for any systems that resemble the oxathiazine oxide ring.

The minor peak (**II**) in the total ion chromatogram shown in Figure 3A is proposed to be mono-GSH adduct **5** (Fig. 4) which

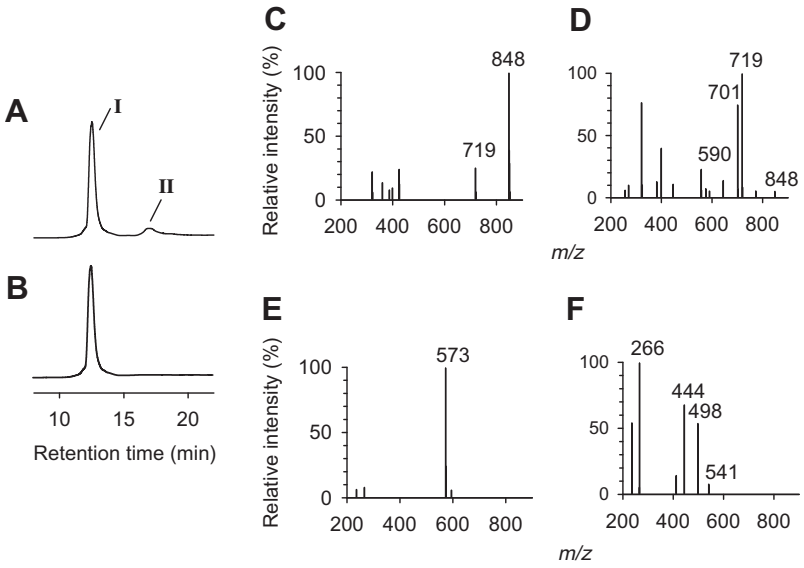

Figure 3. LC–MS/MS characterization of the reaction of bethoxazin with GSH. (A) Total ion chromatogram of the reaction of 100 μM bethoxazin with 2.0 equiv of GSH in the presence of 10% (v/v) methanol as a co-solvent. (B) Total ion chromatogram of the reaction of 100 μM bethoxazin with 2.1 equiv GSH in the absence of methanol. (C) Positive ion mode ESI-MS spectrum of peak **I**. (D) Positive ion mode ESI-MS/MS spectrum of molecular ion *m*/*z* 848. (E) Positive ion mode ESI-MS spectrum of peak **II**. (F) Positive ion mode ESI-MS/MS spectrum of molecular ion *m*/*z* 573.

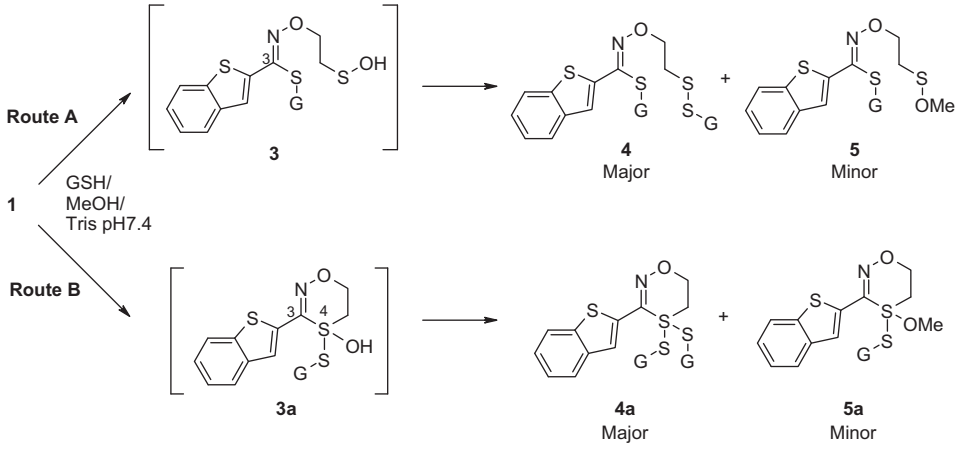

Figure 4. Two possible routes proposed for the reaction of bethoxazin (**1**) with GSH in the presence of methanol as a co-solvent. Route A shows the attack of atom C3 of **1** by GSH to give intermediate **3** which is then attacked at the sulfenic group by a second GSH or the less nucleophilic methanol to give **4** or **5** as a major or a minor product, respectively. Route B shows the attack of GSH at the sulfoxide S4 of **1** to give **3a** that is attacked also at S4 by another GSH or methanol to give **4a** or **5a** as a major or minor product, respectively.

corresponds to molecular ion *m*/*z* 573 identified in the ESI-MS/MS analysis (Fig. 3E). Structure **5a** (Fig. 4), which has the same molecular mass as **5**, is unlikely to be a possible structure for peak **II** as the reaction was reasoned to proceed via intermediate **3**. Daughter ions from MS/MS fragmentation of the molecular ion were *m*/*z* 541, 498, 444 and 266 (Fig. 3F), and likely resulted from the loss of the methoxy, glycyl, glutaryl and glutathionyl groups, respectively, as shown for the fragmentations proposed for structure **5** in Figure 5. The fact that the formation of adduct **5** was only minor even though the concentration of methanol was in large excess (11,000-fold) over the concentration of GSH suggests that its formation was made possible only by the low molar concentration of GSH. Considering that bethoxazin itself did not react with methanol as shown in the spectrophotometric studies, the formation of **5** strongly suggests that intermediate **3** was a much more reactive electrophile than bethoxazin itself. Taken together, Route A of Figure 4 is likely to be the major pathway for nucleophilic attack on bethoxazin.

3.4. ESI-MS characterization of the reaction of bethoxazin with HSA

While bethoxazin was shown to react only slowly with HSA in the spectrophotometric studies, we examined the reaction further using ESI-MS as a model to study the possible sulfhydryl binding of bethoxazin to proteins. The positive ion mass spectra of HSA and HSA treated with bethoxazin are shown in Figure 6A and C, respectively. Since these two spectra show only the *m*/*z* of the multiply charged HSA protein species, molecular mass spectra of neutral proteins were further derived by deconvoluting the protein charge state. Molecular mass spectra for HSA and HSA treated with bethoxazin are shown in Figure. 6B and D, respectively.

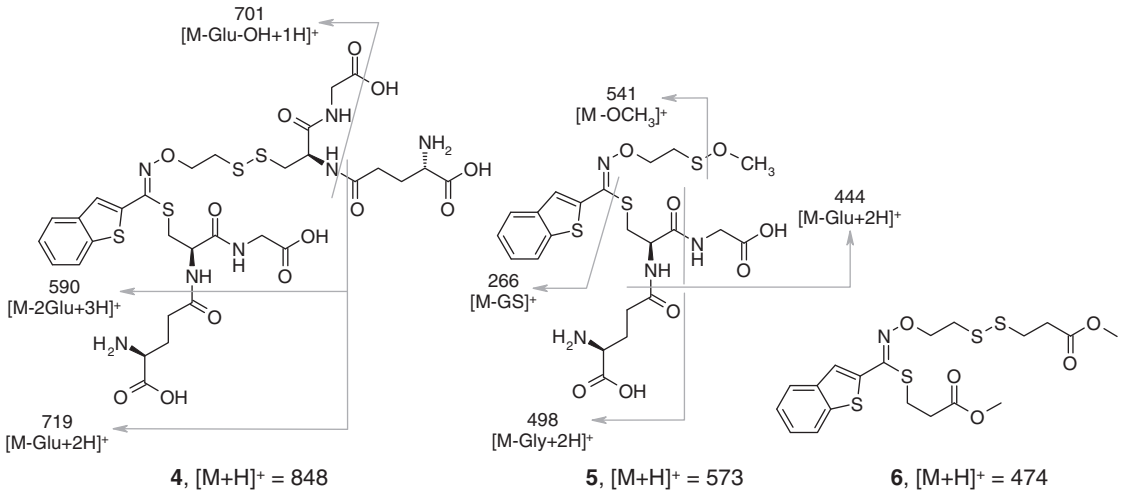

Figure 5. Proposed chemical structures and MS/MS fragmentations of bethoxazin-GSH adducts **4** and **5**, and bethoxazin-methyl 3-mercaptopropionate adduct **6**.

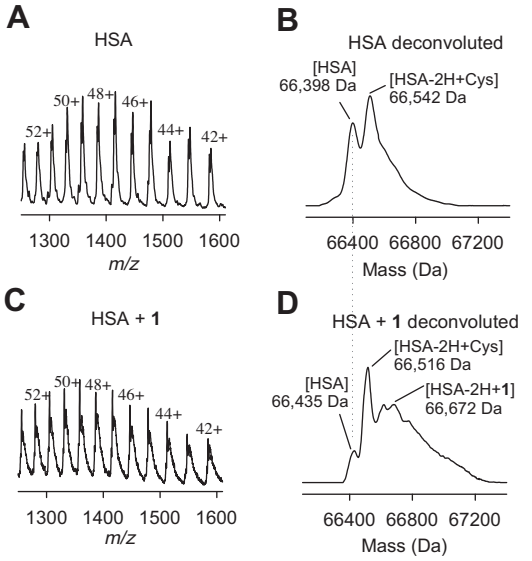

Figure 6. ESI-MS spectra showing covalent labeling of HSA by bethoxazin. Positive ion mode ESI-MS spectra of (A) HSA and (C) HSA treated with bethoxazin at equimolar amount. The numbers above the peaks identify the multiply charged positive ions of the HSA protein species. Deconvoluted molecular mass spectra for (B) HSA and (D) HSA treated with bethoxazin, derived from their corresponding multiply charged protein spectra. Deconvoluted mass spectrum (B) shows that HSA was present as a mixture of free HSA and cysteinylated HSA, whereas (D) shows that treatment with bethoxazin afforded a bethoxazin-HSA adduct.

Commercially available HSA is a mixture of unmodified and post-translationally modified forms.[13] The unmodified free HSA form has a theoretical protonated molecular ion mass of 66439 Da from the amino acid sequence with 17 disulfide bridges and a single Cys-34 residue.[13] The major post-translationally modified form is the cysteinylation form (Cys-HSA) which has a cysteine residue bound to Cys-34 of HSA via a disulfide linkage[13] and has a theoretical molecular ion mass of 66558 Da. The deconvoluted mass spectrum (Fig. 6B) shows that the untreated HSA afforded two major peaks, 66398 and 66542 Da, which corresponded well to the theoretical molecular ion mass of free HSA and Cys-HSA, respectively. The result was consistent with free HSA and Cys-HSA being present in the untreated HSA. After treatment of HSA with one equivalent of bethoxazin, a new peak at 66672 Da appeared in the deconvoluted spectrum as shown in Figure 6D, which was most likely due to formation of mono-HSA adduct of bethoxazin (obsd. **1**-HSA adduct Δm +283 amu; calcd. Δm +251 amu). The result suggests that the reaction of bethoxazin with HSA occurred at an equimolar ratio as opposed to the reactions with small sulfhydryl nucleophiles such as GSH, cysteine, and methyl 3-mercaptopropionate that occurred at RSH–bethoxazin ratio of 2:1. Steric interaction between the bulky mono-HSA adduct of bethoxazin and the partially embedded Cys-34 of a second HSA molecule would be too great for further intermolecular conjugation to take place. Also, the reactive sulfenic group of the mono-HSA adduct would be more likely to react intramolecularly with the neighboring nucleophilic amino acid side chains. Judging by the fact that the peak corresponding to free HSA diminished significantly while the peak corresponding to Cys-HSA was not measurably affected, only the free HSA appeared to have reacted with bethoxazin to form a covalent adduct.

3.5. Effects of bethoxazin, analog 2, and bethoxazin pretreated with GSH on catalytic decatenation activity of purified yeast DNA topoisomerase II and on growth of yeast cells

We and others have shown that the catalytic activity of DNA topoisomerase II enzyme is highly sensitive to sulfhydryl reactive compounds due to the presence of a critical cysteine residue on the enzyme.[14–16] Therefore, topoisomerase II was selected as a model to demonstrate the effects of sulfhydryl binding of bethoxazin on enzymatic catalysis. In addition, given that topoisomerase II is also an enzyme essential for cell growth and division,[17–19] it would be of interest to determine whether bethoxazin may, in part, be exerting its microbicidal action by inhibiting topoisomerase II through reaction with its free sulfhydryl groups. Since yeast cells are frequently used as a model for screening fungicides, we selected yeast BY4742 cell line to study the cytotoxicity of bethoxazin. Given the high reactivity of bethoxazin toward sulfhydryl molecules, reagents containing free sulfhydryl groups, such as DTT and cysteine, were not added in the enzymatic and cell culture assays. However, there was a small amount of DTT (0.2 μM) present in the decatenation assay mixture from the topoisomerase II stock solution. This was much lower than the concentrations of bethoxazin tested and, thus, would only minimally affect the activity of bethoxazin.

The effects of the chemical reactivity of bethoxazin on its enzymatic and cellular activities can be further understood by comparing its activities with those of analog **2**. These two compounds are

structurally so close to each other that any striking difference in their biological activity is likely due to the profound difference in their reactivity toward sulfhydryl binding as shown in the spectrophotometric studies. Given the role of GSH binding as an important physiological detoxification process for many electrophilic xenobiotics, and that this reaction occurred so rapidly for bethoxazin, a bethoxazin sample that had been pretreated with GSH was also included in the enzymatic and cytotoxicity studies to investigate its biological effects.

The inhibition of topoisomerase II catalytic activity was determined by the ability of the compound to inhibit enzyme-mediated decatenation of kDNA into mini circles of DNA that are detectable in an ethidium bromide gel assay (Fig. 7A). In the assay, bethoxazin strongly inhibited the decatenation activity of purified yeast topoisomerase II with an IC_{50} value of 5.3 ± 1 μM (Fig. 7B) even though the reaction was only allowed to proceed at 37 °C for 20 min. The result implies that bethoxazin rapidly reacted with topoisomerase II and that the critical cysteine residues on the enzyme was more readily accessible than that of HSA. In contrast to bethoxazin, analog **2** and bethoxazin pretreated with GSH had no observable effects on the catalytic activity of the enzyme even at 100 μM (Fig. 7A). Consistent with the results obtained for the enzyme assay, bethoxazin also potently inhibited the growth of yeast cells with an IC_{50} value of 11 ± 1 μM, whereas the other two compounds were completely inactive even at 200 μM, as shown in Figure 7C. Notably, the yeast cell growth IC_{50} value obtained for bethoxazin was comparable to its IC_{50} value for topoisomerase II inhibition, suggesting that inhibition of topoisomerase II may be the mechanism by which bethoxazin exerts its cytotoxic effects on yeast cells.

3.6. Computational studies of bethoxazin and analog 2

Since bethoxazin and analog **2** exhibited a striking difference in their reactivity toward sulfhydryl groups despite their close structural resemblance to each other, semi-empirical molecular orbital calculations were carried out to explore whether their properties relating to electrophilicity and reactivity could be correlated with their experimentally observed reactivity. The energy of the highest occupied molecular orbital (E_{HOMO}) and lowest unoccupied molecular orbital (E_{LUMO}) can sometimes predict the nucleophilicity and electrophilicity of a molecule, respectively, with lower E_{LUMO} values implying higher electrophilicity.[20] The absolute difference between E_{HOMO} and E_{LUMO} of a molecule can sometimes serve as a measure of reactivity, where a lower energy gap implies enhanced reactivity due to the ease of excitability.[21] Another method for describing the reactivity of an electrophilic molecule is the widely used global electrophilicity index ($\omega = [E^2_{HOMO} + 2E_{HOMO}E_{LUMO} + E^2_{LUMO}]/[4(E_{LUMO} - E_{HOMO})]$) derived from Koopmans' theorem.[22–24] For this index, a higher value implies greater electrophilicity. The calculated values of these descriptors for bethoxazin and analog **2** shown in Table 1 all suggest that bethoxazin has higher electrophilicity and reactivity than analog **2**, which is in accord with their experimentally observed relative reactivity.

4. Discussion

Bethoxazin and other oxathiazine oxide compounds have a broad spectrum of activity toward different species of microbial organisms.[1,3,4] Although bethoxazin has not been reported to exhibit herbicidal activity, other oxathiazine oxide compounds are known to be herbicidal.[3] Our results showed that the oxathiazine oxide ring of bethoxazin reacted quickly with sulfhydryl nucleophiles. The reaction was pH dependent, suggesting that the thiolate anion was the reactive species. Bethoxazin would be very efficient in its ability to deplete GSH because it reacted with two molecules of GSH. Our results also suggest that the nucleophilic attack of GSH on bethoxazin initially occurred at C3 of the oxathiazine oxide ring, affording intermediate **3** that was even more reactive than bethoxazin itself (Route A of Fig. 4). Even though the reaction of bethoxazin with HSA was slow, the reaction with topoisomerase II was fast, suggesting that there is less steric hindrance at the critical cysteine residues on the enzyme. The potent inhibition of the growth of yeast cells by bethoxazin was also likely due to the reactivity of the compound as demonstrated by the inactivity of its non-reactive analog (**2**) in the same assay. Consistent with our experimental studies, bethoxazin was further shown to be comparatively more electrophilic and reactive than its analog **2** in the quantum mechanical calculations. Like bethoxazin, other electrophilic oxathiazine oxides should also have the ability to deplete GSH concentrations and covalently bind to sulfhydryl enzymes and proteins in the cellular systems. Taken together, we believe that the electrophilic nature of the oxathiazine oxide ring provides a good explanation for the broad spectrum of microbicidal and herbicidal activities exhibited by these compounds. Even though catalytic inhibition of topoisomerase II by bethoxazin may have been sufficient to cause cell death, the reaction with multiple target sites through sulfhydryl binding could be the mechanism by which bethoxazin exerts its microbicidal action and other toxicities.

Woods, plastic, paints, stains and other synthetic materials containing bethoxazin provided excellent outdoor protection against

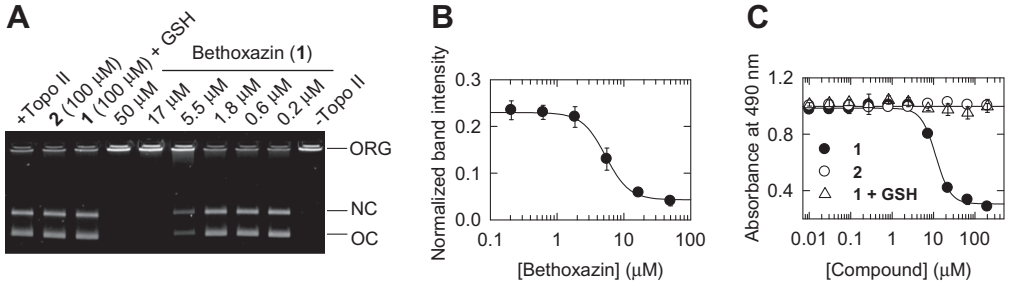

Figure 7. Comparison of the biological activity of bethoxazin, analog **2**, and GSH-treated bethoxazin in the yeast topoisomerase II decatenation and yeast cell culture assays. (A) fluorescent image of the ethidium bromide-stained agarose gel shows that yeast topoisomerase II (+Topo, leftmost lane) decatenated kDNA into nicked (NC) and open (OC) circular DNA. In the absence of the enzyme and compound (-Topo II, rightmost lane), kDNA stayed in the origin (ORG). At 100 μM, analog **2** and bethoxazin sample pretreated with 2.1 equivalents of GSH did not have any effect on the decatenation activity of the enzyme. However, bethoxazin itself inhibited the enzyme in a concentration dependent manner. (B) The potency of bethoxazin on topoisomerase II decatenation inhibition was measured by densitometric quantification of combined band intensities of NC and OC at various concentrations of bethoxazin from two separate gels, normalized to a value of 0.22 in the absence of bethoxazin. Bethoxazin inhibited the enzyme with an IC_{50} value of 5.3 ± 1 μM. (C) The growth inhibitory effects of bethoxazin (●), analog **2** (○), and bethoxazin pretreated with 2.1 equiv of GSH (△) on yeast BY4742 cells as measured by an MTS assay with three replicates for each drug. Bethoxazin inhibited the growth of yeast cells with an IC_{50} value of 11 ± 1 μM, whereas analog **2** and GSH-treated bethoxazin were inactive even at 200 μM. The solid lines in (B) and (C) are nonlinear least square fits to a four-parameter logistic equation. Where the error bars are not shown, they are smaller than the symbol.

Table 1
HOMO and LUMO energy levels calculated for bethoxazin and analog **2**

	Bethoxazin	**2**
E_{HOMO} (eV)	−8.726	−8.795
E_{LUMO} (eV)	−1.321	−0.990
$\lvert E_{HOMO} - E_{LUMO} \rvert$ (eV)	7.405	7.763
ω (eV)	3.408	3.060

These values were used to calculate the absolute difference of the energy levels ($\lvert E_{HOMO} - E_{LUMO} \rvert$) and global electrophilicity index (ω).

wood and material decay organisms such as algae, fungi and molds.[1] These materials consist of unreactive polymeric matrices and also do not contain any nucleophilic detoxification systems that are present in living organisms. Although woods are derived from plants, they are composed mainly of cellulose fibers embedded in lignin polyphenolic matrices, both of which lack any free sulfhydryl groups. In addition, the phenolic protons of lignin contribute to an acidic environment (average pH of 5) in wood,[25] which would be a pH range favorable for maintaining the stability of bethoxazin.[1] The reactivity profile that we showed for bethoxazin adds to a better understanding of why bethoxazin is suitable for use as a preservative for industrial materials, and may help define conditions for other practical applications of this compound.

Bethoxazin is relatively non-toxic to rats in the acute oral and dermal LD_{50} toxicity tests, but highly toxic in the inhalation toxicity test.[1] In addition, it also causes moderate and severe irritation to the skin and eyes on rabbits, respectively.[1] The favorable toxicological profile of bethoxazin in the acute oral toxicity tests can be explained by a number of factors. Given the reactivity of bethoxazin toward sulfhydryl groups, the molecule would be susceptible to GSH conjugation in first-pass metabolism when administered orally in rats. Our topoisomerase II and yeast cell culture studies showed that GSH conjugation rendered bethoxazin inactive. Therefore, it is anticipated that the first-pass metabolism in rats would deactivate bethoxazin. The high acute oral LD_{50} value of 3631 mg/kg obtained for bethoxazin in rats[1] is comparable to that of acetaminophen (1944 mg/kg in rats, MSDS, Acros, Fair Lane, NJ), in which its reactive metabolite is known to be detoxified by conjugation with GSH.[26–28]

Given its stability under UV and at high temperature,[1] bethoxazin should remain stable on plant foliar surfaces in the testing environment. However, bethoxazin is likely absorbed into the underlying tissue of plants because it has a log octanol–water partition coefficient value of 2.7,[1] which is in the range considered optimal for plant systemic uptake.[29] Since plant cells, like microbial and animal cells, contain high concentrations of GSH for the detoxification of xenobiotics,[30,31] bethoxazin would be rapidly deactivated in plants by conjugation with GSH. The reactivity profile of bethoxazin provides a convincing explanation for the failure of bethoxazin to act as a fungicide for crop protection applications.

In summary, our studies have provided for the first time a better understanding of the chemical reactivity of bethoxazin and the oxathiazine oxide ring, and how its reactivity defines the biological activities and practical applications of this compound.

Acknowledgments

This work was supported by Chemtura Corporation (formerly Crompton, Uniroyal Chemical, and Great Lakes), institutional grants from the University of Manitoba and Canadian Institutes of Health Research, and a Canada Research Chair in Drug Development for B.B.H.

Supplementary data

Supplementary data associated with this article can be found, in the online version, at doi:10.1016/j.bmc.2011.12.051.

References and notes

1. Bosselaers, J.; Blancquaert, P.; Gors, J.; Heylen, I.; Lauwaerts, A.; Nys, J.; Van der Flaas, M.; Valcke, A. *Faerg och Lack Scandinavia* **2003**, *49*, 5.
2. Nichols, D. *Rapra Review Report* **2004**, *15*, 24.
3. Brouwer, W. G.; Bell, A. R.; Blem, R.; Davis, R. A. U.S. Patent 4,569,690, 1986.
4. Davis, R. A.; Valcke, A.; Brouwer, W. G. 5777110, July 7, 1998, U.S. Patent 5,777,110, 1998.
5. Gallagher, J. F.; Ferguson, G.; Brouwer, W. G. *Acta Crystallogr., Sect. C* **1997**, *53*, 823.
6. Van Gestel, J. F. E. U.S. Patent 5,712,275, 1998.
7. Wallace, D. F.; Dickinson, D. J. Int. Res. Group Wood Preservation 35th Annu. Meeting (Slovenia) 2004, 04.
8. Balta, B.; Monard, G.; Ruiz-López, M. F.; Antoine, M.; Gand, A.; Boschi-Muller, S.; Branlant, G. *J. Phys. Chem. A* **2006**, *110*, 7628.
9. Smith, S. G.; Winstein, S. *Tetrahedron* **1958**, *3*, 317.
10. Nitiss, J. L.; Liu, Y.-X.; Harbury, P.; Jannatipour, M.; Wasserman, R.; Wang, J. C. *Cancer Res.* **1992**, *52*, 4467.
11. Hasinoff, B. B.; Creighton, A. M.; Kozlowska, H.; Thampatty, P.; Allan, W. P.; Yalowich, J. C. *Mol. Pharmacol.* **1997**, *52*, 839.
12. Aversa, M. C.; Barattucci, A.; Battaglia, G.; Bonaccorsi, P. *Phosphorus, Sulfur Silicon* **2011**, *186*, 1220.
13. Kleinova, M.; Belgacem, O.; Pock, K.; Rizzi, A.; Buchacher, A.; Allmaier, G. *Rapid Commun. Mass Spectrom.* **2005**, *19*, 2965.
14. Gantchev, T. G.; Hunting, D. J. *Mol. Pharmacol.* **1998**, *53*, 422.
15. Hasinoff, B. B.; Wu, X.; Krokhin, O. V.; Ens, W.; Standing, K. G.; Nitiss, J. L.; Sivaram, T.; Giorgianni, A.; Yang, S.; Jiang, Y.; Yalowich, J. C. *Mol. Pharmacol.* **2005**, *67*, 937.
16. Wu, X.; Liang, H.; O'Hara, K. A.; Yalowich, J. C.; Hasinoff, B. B. *Chem. Res. Toxicol.* **2008**, *21*, 483.
17. Figgitt, D. P.; Denyer, S. P.; Dewick, P. M.; Jackson, D. E.; Williams, P. *Biochem. Biophys. Res. Commun.* **1989**, *160*, 257.
18. Gasser, S. M.; Walter, R.; Dang, Q.; Cardenas, M. E. *Int. J. Gen. Mol. Microbiol.* **1992**, *62*, 15.
19. Nitiss, J. L. *Nat. Rev. Cancer* **2009**, *9*, 327.
20. Fleming, I. *Molecular Orbitals and Organic Chemical Reactions: Reference Edition*; John Wiley and Sons, Ltd: West Sussex, UK, 2010.
21. Vittori, S.; Mishra, R. C.; Dal Ben, D.; Kachare, D.; Lambertucci, C.; Volpini, R.; Cristalli, G. *Nucleosides, Nucleotides Nucleic Acids* **2007**, *26*, 1439.
22. Chattaraj, P. K.; Roy, D. R. *Chem. Rev.* **2007**, *107*, PR46.
23. Parr, R. G.; Szentpály, L. V.; Liu, S. *J. Am. Chem. Soc.* **1999**, *121*, 1922.
24. Schwöbel, J. A. H.; Wondrousch, D.; Koleva, Y. K.; Madden, J. C.; Cronin, M. T. D.; Schüürmann, G. *Chem. Res. Toxicol.* **2010**, *23*, 1576.
25. Landi, L.; Staccioli, G. *Eur. J. Wood Wood Products* **1992**, *50*, 238.
26. Calder, I. C.; Creek, M. J.; Williams, P. J.; Funder, C. C.; Green, C. R.; Ham, K. N.; Tange, J. D. *J. Med. Chem.* **1973**, *16*, 499.
27. Kunkel, D. B. *Emergency Medicine. Geigy Pharmaceuticals* 1985, July 15.
28. Lemke, T. L.; Williams, D. A. *Foye's Principles of Medicinal Chemistry*; Lippincott Williams & Wilkins: Baltimore, MD, 2008.
29. Edgington, L. V. *Annu. Rev. Phytopathol.* **1981**, *19*, 107.
30. Cummins, I.; Dixon, D. P.; Freitag-Pohl, S.; Skipsey, M.; Edwards, R. *Drug Metab. Rev.* **2011**, *43*, 266.
31. Soleo, L.; Strzelczyk, R. *Giornale italiano di medicina del lavoro ed ergonomia* **1999**, *21*, 302.